PERFORMANCE OF THE ANTARES LARGE AREA COLD CATHODE ELECTRON GUN*

L. A. Rosocha and C. R. Mansfield

Los Alamos National Laboratory
P. O. Box 1663
Los Alamos, New Mexico 87545

Summary

The performance of the electron gun which supplies ionization for the Antares high power electron beam sustained CO_2 laser power amplifier is described. This electron gun is a coaxial cylindrical cold cathode vacuum triode having a total electron aperture area of approximately 9 m^2. Electrons are extracted from the gun in pulses of 3-6 μs duration, average current densities of 40-60 mA/cm^2, and electron energies of 450-500 keV. The main areas of discussion in this paper are the performance in terms of grid control, current density balance, and current runaway due to breakdown limitations. Comparison of the experimental results with the predictions of a theoretical model for the electron gun will also be presented.

Introduction

Antares is a high power gas laser system being constructed for inertial confinement fusion studies. The Antares system and the main power amplifiers have been previously described by Jansen[1] and by Stine, et al[2] in terms of mechanical, electrical, and optical design. The heart of the laser system consists of two large aperature electron beam sustained CO_2 laser amplifiers having a stage gain of approximately 200 with an optical output energy of 15-20 kJ per amplifier. Each amplifier has four separate anodes which are pulsed to nearly 550 kV in 4-6 μs. Each of these anodes excites 12 identical volumes of CO_2/N_2 laser gas, these volumes being about 75 cm long and of nearly trapezoidal cross-section with an area of approximately 1200 cm^2. The electron gun supplies ionization for all of these gas volumes prior to and during the application of the main anode voltage excitation pulses.

Design considerations for the Antares electron gun have been treated by Scarlett, et al[3]. There are three main design constraints: these are: sufficient electron energy to penetrate the Kapton-aluminum exit windows and the laser gas between the windows and the power amplifier anodes, sufficient electron current density magnitude and uniformity so proper impedance matching to the anode discharge is obtained and so an adequately uniform distribution of active laser gain region will also be obtained, and minimal electric field enhancement at the electrodes so vacuum breakdown and current runaway is avoided.

The final configuration of the Antares electron gun is a coaxial cylindrical cold cathode vacuum triode with cathode, grid, and anode (ground) diameters of 104, 130, and 159.5 cm, respectively and an approximate length of 7.7 m for the anode shell. The anode shell, which is also the vacuum vessel, is penetrated by 48 electron exit windows of dimensions 25x75 cm, each window opening having 0.8 cm thick hibachi ribs spaced on 6.3 cm centers for mechanical strength of the vacuum vessel and support of the electron windows. The actual exit windows are a Kapton-aluminum laminate (2 mil each) bonded to a 1 mm (40 mil) thick stainless steel support grid. The grid is constructed from 4.76 mm (3/16") diameter stainless steel rod or tube stock. This grid material is either made into hoops of the major grid diameter and spaced 2.54 cm (1") apart along the long axis of the gun or wound around the major diameter of the grid as a helix with a 2.54 cm (1") pitch. The cathode is an aluminum cylinder to which 48 emitter blades of 12.7 μm (0.5 mil) tantalum foil 75 cm in length are attached in four groups of twelve blades which are symmetrically spaced around the circumference of the cathode. Figure 1 shows the basic geometry of the Antares E-gun.

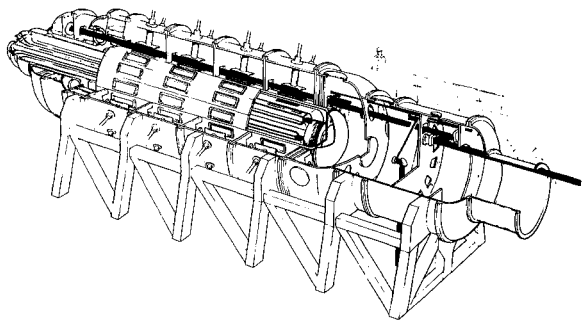

Figure 1: Cutaway illustration of the Antares power amplifier showing the cylindrical electron gun in the center. The rectangular structures on the surface of the E-Gun are the electron beam exit ports. Each group of twelve windows is surrounded by a torus-shaped anode which is pulsed to excite the laser gas.

In operation, the electron gun is connected to a 10 stage Marx generator which pulses the cathode to about 0.5 MV. When the blade ignition voltage is reached, field emission at the blade tips results in cathode current flow which, for a diode, would be ultimately limited by space-charge effects. However, our E-gun is a triode with the grid connected to the anode by means of a biasing resistor. The flow of grid current through this resistor provides a voltage between the grid and cathode which results in control of the cathode current. There are two principal advantages of this grid-controlled E-gun. The first is that the cathode current can be regulated by means of the grid biasing resistor, independent of the anode-cathode voltage and the electrode spacings. The second advantage is that the grid will tend to stabilize the cathode current, i.e. an increase in cathode current will lead to an increase in grid bias thus cutting off the emission of cathode current. This stabilization will occur as long as the electric field at the grid surface is low enough so that the grid does not emit electrons and become a secondary cathode. Figure 2

*Work performed under the auspices of the U. S. Department of Energy

Report Documentation Page

Form Approved
OMB No. 0704-0188

1. REPORT DATE	2. REPORT TYPE	3. DATES COVERED
JUN 1983	**N/A**	**-**

4. TITLE AND SUBTITLE	5a. CONTRACT NUMBER
Performance Of The Antares Large Area Cold Cathode Electron Gun	5b. GRANT NUMBER
	5c. PROGRAM ELEMENT NUMBER
6. AUTHOR(S)	5d. PROJECT NUMBER
	5e. TASK NUMBER
	5f. WORK UNIT NUMBER
7. PERFORMING ORGANIZATION NAME(S) AND ADDRESS(ES) **Los Alamos National Laboratory P. 0. Box 1663 Los Alamos, New Mexico 87545**	8. PERFORMING ORGANIZATION REPORT NUMBER
9. SPONSORING/MONITORING AGENCY NAME(S) AND ADDRESS(ES)	10. SPONSOR/MONITOR'S ACRONYM(S)
	11. SPONSOR/MONITOR'S REPORT NUMBER(S)

12. DISTRIBUTION/AVAILABILITY STATEMENT
Approved for public release, distribution unlimited

13. SUPPLEMENTARY NOTES
See also ADM002371. 2013 IEEE Pulsed Power Conference, Digest of Technical Papers 1976-2013, and Abstracts of the 2013 IEEE International Conference on Plasma Science. Held in San Francisco, CA on 16-21 June 2013. U.S. Government or Federal Purpose Rights License.

14. ABSTRACT

15. SUBJECT TERMS

16. SECURITY CLASSIFICATION OF:			17. LIMITATION OF ABSTRACT	18. NUMBER OF PAGES	19a. NAME OF RESPONSIBLE PERSON
a. REPORT	b. ABSTRACT	c. THIS PAGE			
unclassified	**unclassified**	**unclassified**	**SAR**	**4**	

is an electrical circuit schematic for the electron gun and its associated Marx generator.

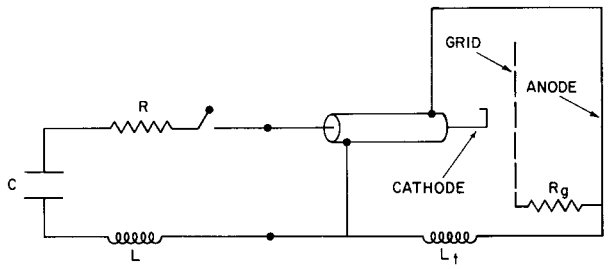

Figure 2: Electrical schematic diagram for the electron gun and associated Marx generator. The E-gun is fed by a triaxial transmission line arrangement to minimize magnetic effects. The cathode current can return to the Marx through a ground return line in the center of the electron gun or through the E-gun shell and balance inductor. The Marx parameters are C = 0.375 uF, L = 3.0 μH, R = 3.0 ohms; the balance inductor is in the range 1 - 6 μH.

Measured Performance: Cathode Voltage and Current

We have completed performance and check-out testing on three Antares electron guns; all three E-guns are essentially identical in geometry and dimensions except that an earlier design used a punched sheet metal grid of 0.8 mm (1/32") thickness rather than the present design of rod or tube stock. The voltage hold-off of the earlier grid design was considerably less than the present design, resulting in unreliable performance. We will only present data for the performance of E-guns using the improved grid design in this paper. The two electron guns were successfully tested and characterized for a typical range of cathode voltage of 446 ± 31 kV to 507 ± 35 kV. A diverter switch was used to cut off the pulse width at a predetermined value of from 2.5 μs to 6.0 μs. The E-guns were brought on line and conditioned up to working voltage by raising the Marx charge voltage in conjunction with widening the Marx voltage pulse width. In the operating range of interest, the E-gun impedance was about 15-25 ohms. One E-gun has a slightly smaller impedance (1-2 ohms) than the other: this may be due to a slight difference in emitter blade structure between the two E-guns. Figure 3 shows an example of some typical results for our measurements of cathode voltage and cathode current waveforms. The E-gun parameters associated with these waveforms are listed in the figure caption. Several other voltages and currents are also measured during typical E-gun operations; these are: Marx output voltage, grid voltage, grid current, total return current, and anode return current. Due to space limitations, we do not display all of these in this paper.

In addition to the cathode voltage and current, we have determined E-gun performance in terms of absolute measurements of emitted electron current density. The probes which monitor the emitted current are Faraday plates having an area of 1,000 cm^2, or about one-half of the Kapton-aluminum window area. These plates were placed about 2 cm outside and parallel to the plane of the windows to intercept the emitted electrons; the plates were then coupled to ground through current transformers which gave an output voltage proportional to the electron current density. Fig. 4 shows plots of temporally-averaged current density as a function of E-gun longitudinal position for typical cathode voltages and grid resistor values. The emitted electron current density varies with longitudinal position since current flowing in the cathode creates an azimuthal magnetic field which causes deflections in the trajectory of the emitted electrons. Magnetic effects are reduced in the Antares E-gun design by feeding the cathode from both ends in a symmetrical manner. A tuning inductor placed in one of the return current transmission lines provides a means of adjusting the longitudinal variation in the electron current density. Fig. 5 shows results of adjusting the distribution by means of this tuning inductor.

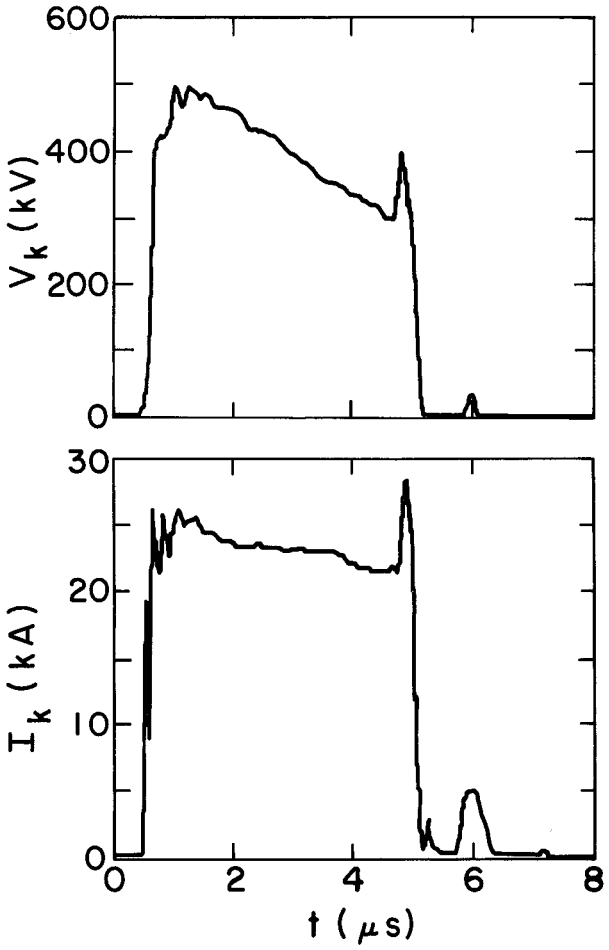

Figure 3: Typical measured cathode voltage and cathode current waveforms. The Marx charge voltage was 57 kV, the grid resistor was 150 ohms, and the balancing inductor was about 3 μH.

The Faraday probes give good temporal resolution for the output current density of the electron gun but only poor spatial resolution of the distribution of current densities. Two techniques have been employed to study the spatial distribution of current density. In the Cherenkov technique 5-10 mm acrylic plates are placed over the foil windows. The Cherenkov radiation produced by the high energy output electrons is then photographed on high speed photographic film. The detailed spatial current

density distribution of up to 12 windows can be recorded during a shot on one photographic record.

Production of x-rays by the high energy electrons has been used to study both the distribution across a window opening when the Kapton-aluminum window has been replaced by a 7 mm steel plate and to explore the current density distributions at the inner surface of the anode. This latter distribution is of some interest in that the electron gun produces a nearly uniform azimuthal distribution at the inner surface of the anode with virtually no electrons striking the anode between the windows in a direction along the length of the electron gun.

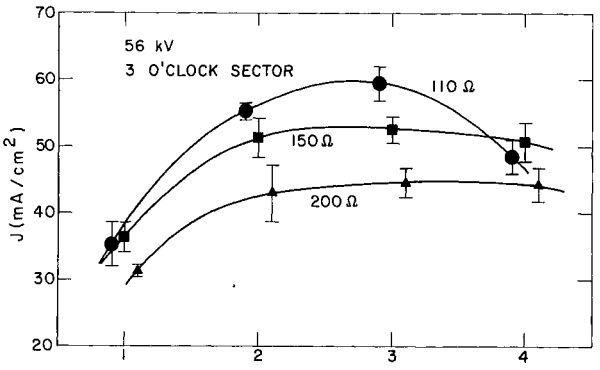

Figure 4: Example of some typical measurements of the emitted electron current density for three different values of grid resistor. The values of J shown are temporal averages (i.e. square-wave equivalent) of the current density. These measurements are for one of twelve sector positions; the anode position along the length of the electron gun is indicated by the 1-4 label, with position 1 being closest to the Marx. This particular window position has a low output in Section 1.

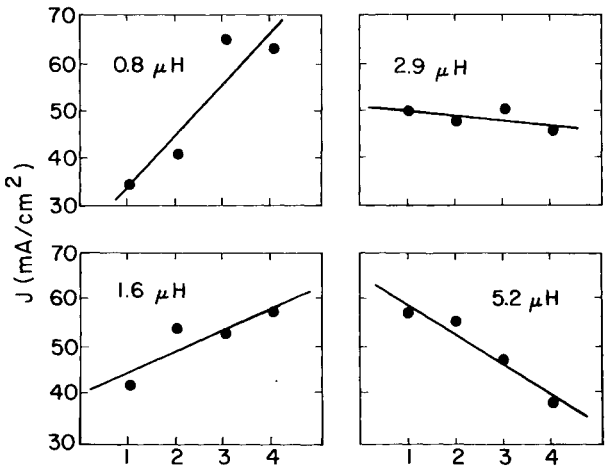

Figure 5: Plots of the emitted electron current density vs. electron gun longitudinal position for four different values of balancing inductor. The best balance is achieved with a 2.9 μH inductor when the E-gun is in our test bay. With the E-gun in the power amplifier, the value is larger (6 μH) due to somewhat different grounding within the power amplifier.

Measured Performance: Breakdown Limitations

One of the most serious limitations on E-gun performance is the peak electric field stress at the surface of the grid electrode. Calculations of the electric stress by means of a numerical solution to Laplace's equation for the Antares electron gun geometry have shown that the peak stress for a punched metal grid is about 3 times the mean stress, whereas for a tube or rod grid, the peak stress is only about 2 times the mean stress[4]. Our measurements of the performance of E-guns using both types of grids agree with the calculations in that reliable performance of the E-Gun with the punched metal grid was limited to cathode voltages of < 400 kV, while the E-guns with the rod or tube grids showed reliable performance above 500 kV cathode voltages. These cathode voltages correspond to values of average grid-anode electric field hold-off of about 25 kV/cm for the punched metal grid and 31 kV/cm for the rod or tube grids.

Performance limitations are also imposed by the hold-off voltage of the electron gun high voltage bushings, particularly the grid-anode bushing. Flashover of this bushing can lead to massive cathode curent runaway. We have found that proper quality control in the manufacture of this bushing (e.g., elimination of sharp points and leftover globules from the epoxy bond) will enable the bushing to perform in accordance with its design specifications[5].

Degredation of the E-gun vacuum will also lead to reduced performance through low pressure gas breakdown phenomena inside the electron gun. We have deliberately added pure N_2 to the E-gun to identify the regime in which poor vacuum adversely affects performance. A rough criterion for the onset of cathode current instability with a N_2 additive is a pressure in the range of 0.8 - 1.0 x 10^{-4} torr for peak cathode voltages in the range 475 - 500 kV.

We have some indications that hydrogen is a particularly bad contaminent to the electron gun. There are several potential sources of hydrogen in the E-gun. The main sources are hydrocarbons such as oil, vacuum grease, bushing material and water adsorbed on the surface of the vacuum chamber. These materials are broken down by electron bombardment during a shot. The pressure pulse on a typical shot is about 1×10^{-5} torr with a "clean" gun. When the gun is badly contaminated with oil the pulses, monitered near the vacuum pumps, can approach 10^{-4} torr.

The mechanism behind the performance degradation is not well understood. In part it was related to the use of the old style punched metal grid which was mentioned earlier. In that case, the higher field stresses on the grid led to emission of electrons at the grid and the generation of a hydrogen plasma which could quickly close the grid cathode gap. By strict cleaning and use of silicon vacuum greases it was possible to raise the operating cathode voltage of the gun with an old-style grid from 400 kV to 450 kV.

Experiment/Theory Comparisons

The Antares electron gun operation is theoretically described by the concepts of field emission and the Langmuir-Child space-charge limited diode model. A steady state solution for a vacuum triode having cylindrical geometry is described by the following relation between the cathode voltage and the cathode current[6]

$$I_k = 14.68\times10^{-6}\left[V_k-(1-T)R_g\right]^{3/2}(1/r_g\beta^2), \qquad (1)$$

where I_k is the cathode current, V_k is the cathode voltage, R_g is the grid resistance, T is the grid transmission, r_g is the grid radius, l is the cathode length, and β is a function of the grid radius to cathode radius ratio r_g/r_c. If we substitute the Antares electron gun parameters of r_g = 65 cm, r_c = 52 cm, and $\beta \simeq 0.2$ into Equation 1 and do some algebraic manipulation, we can get the following relation for the E-gun impedance Z

$$Z = V_k/I_k = (1-T)R_g + 63.4\ I^{-1/3}. \qquad (2)$$

In the operating range of interest for the Antares electron gun, the cathode current is about 15-30 kA. The second factor in the above equation varies by only about 0.5 ohms over this range, so in presenting our results we will set the second factor in Equation 2 equal to the average value over the range of interest, namely 2.3 ohms. Fig. 6 shows a plot of our measured values of E-gun impedance compared to the results calculated by means of Equation 2. In the calculations, we have used the measured value for the grid transmission 0.87, rather than the geometrical grid transmission of 0.80. The agreement between calculation and measurement is reasonable considering that we have applied a steady state model to an intrinsically transient phenomenon.

Further theoretical modelling of the Antares electron guns has been done by Leland and Kircher[7]. This work has dealt with predicting the electrical behavior of the electron gun by means of a computer-based, time-dependent model in which the E-gun is described as a distributed electrical system coupled to a lumped-parameter Marx driving circuit. The electron emission from the blades is treated by a transient Langmuir-Child diode theory. This model predicts cathode voltage and current waveforms that are in reasonable agreement with the measurements reported in this paper.

Conclusions

Our measurements of the performance of the present design of the Antares electron guns have shown that the present E-guns can adequately meet the power amplifier operational requirements of electron energies of 450-500 keV and emitted electron current densities of 40-50 mA/cm^2. The electron gun designs which incorporate tubular or rod grids are more reliable than designs utilizing punched metal grids since the electric field enhancement is less for the rod or tube grids. The measured performance is in reasonable agreement with both a steady state Langmuir-Child diode model and a more detailed time-dependent computer model for the electron gun coupled to its driving electrical circuit.

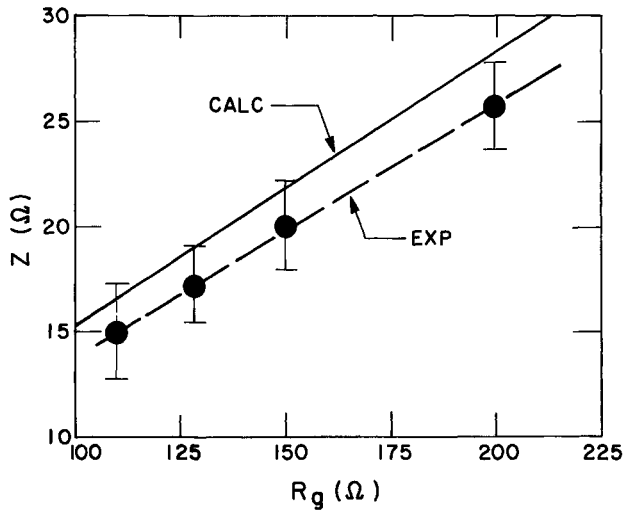

Figure 6: Electron gun impedance plotted as a function of grid resistor. The solid curve shows values of Z calculated by means of Equation 2, while the dots are values derived from our measurements of cathode voltage and current. For our measured values, we chose V_k and I_k at one particular time on the measured waveforms (viz. 2.0 μS).

References

1. J. Jansen, "Review and Status of Antares", Proc. of 2nd Int. IEEE Pulsed Power Conf., Lubbock, Texas, June 12-14, 1979, p. 31.

2. R. D. Stine, G. F. Ross, and C. Silvernail, "The Antares Laser Power Amplifier", Proc. of 2nd Int. IEEE Pulsed Power Conf., Lubbock, Texas, June 12-14, 1979, p. 265.

3. W. R. Scarlett, K. R. Andrews, and J. Jansen, "A Large-Area Cold-Cathode Grid-Controlled Electron Gun for Antares", Proc. of 2nd Int. IEEE Pulsed Power Conf., Lubbock, Texas, June 12-14, 1979, p. 261.

4. E. Jolly and F. Van Haaften, "Field Plots of Antares E-gun", Internal Memo P-7/82-239, Los Alamos National Laboratory, May 28, 1982 (unpublished).

5. R. D. Stine, G. R. Allen, E. Eaton, and B. Weinstein, "Bonded Stacked Ring Insulator for the Antares Electron Gun", Ann. Rep. Conf. on Electrical Insulation and Dielectric Phenomena, Amhurst, Mass., Oct. 17-21, 1982, p. 524.

6. I. Langmuir and K. Blodgett, "Currents Limited by Space Charge between Coaxial Cylinders", Phys. Rev., 22, 347 (1923).

7. W. Leland and M. Kircher, "Antares Gun Modeling", Los Alamos National Laboratory internal report, LA-UR-82-1088, 1982 (unpublished).

Acknowledgment

The authors would like to thank Kenneth Andrews for his assistance in carrying out the measurements reported in this paper.